Precipitation of Oppositely Charged Nanoparticles by Dilution and/or Temperature Increase

Kyle J. M. Bishop, Bartlomiej Kowalczyk, and Bartosz A. Grzybowski*

Department of Chemical and Biological Engineering and Department of Chemistry, Northwestern University, 2145 Sheridan Rd., Evanston, Illinois 60208

Received: June 26, 2008; Revised Manuscript Received: November 24, 2008

Mixtures of oppositely charged nanoparticles (NPs) exhibit anomalous solubility behavior and precipitate either upon dilution or upon temperature increase. Precipitation is reversible and can be explained by a thermodynamic model that accounts for changes in the electrostatic interactions due to the adsorption/desorption of counterions from the surface of the NPs. Specifically, decreasing the salt concentration via dilution or increasing the temperature causes dissociation of counterions from the NP surfaces, increasing the magnitude of electrostatic interactions between NPs and resulting in their precipitation. Model predictions of NP solubility are in quantitative agreement with the experimental observations. Such predictions are of practical importance for the preparation of "patchy" electrostatic coatings and ionic-like NP supracrystals.

Introduction

Dissolution of simple molecular or ionic solids can almost always be achieved by increasing either the volume of the solvent or the temperature of the system. On the other hand, in some types of complex fluids dilution and/or heating may instead result in aggregation and precipitation of the dissolved species. For example, mixtures of proteins and ionic surfactants may aggregate/precipitate upon dilution with water due to the desorption of stabilizing surfactants from the protein surface.[1] Similarly, an increase in temperature may result in the precipitation of some proteins[2] or polymers[3] from aqueous solutions due either to the disruption of stabilizing hydration layers[4] or to conformational changes that increase the hydrophobic character of the macromolecules.[3] Here, we describe a conceptually different system, in which precipitation upon either dilution or temperature increase results not from conformational changes but from "unmasking" of electrostatic interactions between the system's nanoscopic components. This system comprises oppositely charged nanoparticles (NPs) suspended[5] in an aqueous electrolyte solution. Owing to the nanoscopic dimensions of the particles, the van der Waals interactions between these NPs are weak, and because the attractive electrostatic interactions are effectively screened, the system is thermodynamically stable against aggregation. A decrease in salt concentration upon dilution or an increase in temperature, however, shifts the equilibria governing the adsorption of counterions onto the NP surfaces, thereby increasing the magnitude of interparticle electrostatic forces and causing the NPs to precipitate. These effects are captured by a theoretical model, which, in a wider context, illustrates the importance of counterion surface equilibria in describing interactions between charged nano-objects. The precipitation effects reported in this paper might have practical consequences for the preparation of stable solutions of charged NPs that are used for the preparation of "patchy" electrostatic coatings[6] and ionic-like NP supracrystals.[7−9]

* Corresponding author. E-mail: grzybor@northwestern.edu.

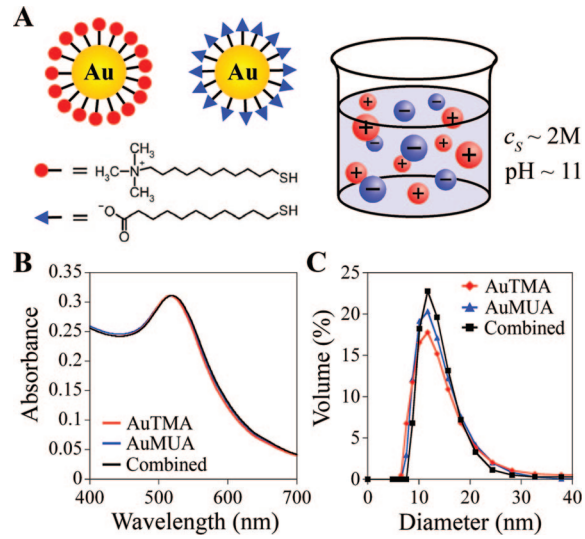

Figure 1. (A) Scheme of positively charged AuTMA NPs (red) and negatively charged AuMUA NPs (blue). At high salt concentrations ($c_S \sim 2M$), 1:1 mixtures of equally sized, oppositely charged NPs can be dissolved completely in aqueous solution. (B) UV−vis extinction spectra of the NP mixtures (black) are nearly identical to those of "pure" AuTMA (red) and AuMUA (blue) solutions of equal concentration. (C) Likewise, DLS experiments reveal that the hydrodynamic diameters of the NP mixtures agree well with those of the constituent particles. These results indicate that oppositely charged NPs are free and unaggregated in solution.

Experimental Details

Our experiments were based on aqueous solutions of $N(CH_3)_4Cl$ salt ($c_S \sim 1-2$ M; with pH adjusted to 11 by addition of $N(CH_3)_4OH$) containing approximately equal numbers of equally sized (either 5.9 ± 0.7, 7.1 ± 0.8, or 11 ± 1.1 nm in diameter), oppositely charged, gold nanoparticles (NPs; Figure 1A).[7,10] Positively charged AuNPs were coated with *N*,*N*,*N*-trimethyl(11-mercaptoundecyl)ammonium chloride (TMA, ProChimia Surfaces);[10] negatively charged NPs were covered with a SAM of deprotonated mercaptoundecanoic acid (MUA, ProChimia Surfaces; pK_a in NP/SAM ca. 6−8[10−12]). As de-

10.1021/jp8056493 CCC: $40.75
Published on Web 01/08/2009

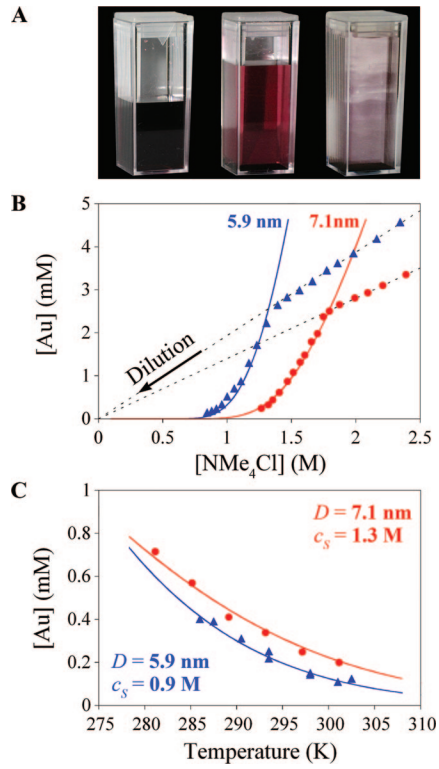

Figure 2. (A) Dilution-induced precipitation of oppositely charged NP mixtures. The NP concentration (reflected by the intensity of the solution's reddish hue) decreases with increasing dilution due to precipitation and subsequent sedimentation of NP aggregates. After diluting two times, the NPs are almost completely precipitated. (B) Concentration of NPs (in terms of gold atoms and quantified by UV−vis) as a function of salt concentration during dilution experiments using 5.9 nm (blue triangles) and 7.1 nm (red circles) NPs at 298 K. Initially, the concentration decreases linearly, as expected for dilution *without* precipitation. Upon intersection with the theoretically calculated solubility curve (solid curves), precipitation ensues, and the data trace the equilibrium NP solubility curve. Data for larger 11 nm particles are not shown as these particles were insoluble at all salt concentrations. (C) Concentration of NPs (in terms of gold atoms) as a function of temperature for 5.9 nm (at salt concentration, $[NMe_4Cl] = 0.9$ M) and for 7.1 nm ($[NMe_4Cl] = 1.3$ M). Again, the solid markers represent experimental measurements, and the curves are the theoretically calculated solubility. NPs precipitate with increasing temperature.

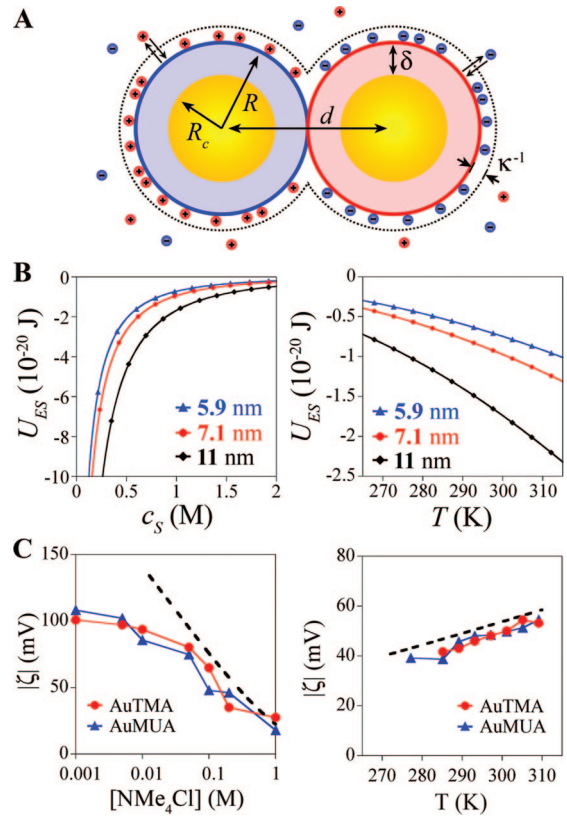

Figure 3. (A) Scheme of two interacting, oppositely charged NPs at contact. (B) Dependence of the electrostatic interaction energy on both salt concentration (left, for $T = 298$ K) and temperature (right, for $c_S = 0.9$ M) using best-fit parameters given in the main text. (C) Absolute value of the ζ-potential for positively charged TMA-NPs (diameter = 7.1 nm, red circles) and negatively charged MUA-NPs (diameter = 7.1 nm, blue triangles) as a function of salt concentration (at 298 K) and temperature (at 0.2 M salt), respectively. The black curve is the surface potential of an isolated particle as calculated by the model presented in the text and using the best-fit value of $\Delta G_d \approx 2.1 \times 10^{-20}$ J. In both cases, the model overestimates the ζ-potential by a few millivolts likely because it does not account for the precise location of the surface of shear (surface potentials were calculated at the NP surface). Furthermore, in the case of salt concentrations less than ~0.1 M the model is inappropriate due to the failure of the linearization of the Poisson−Boltzmann equation.

scribed previously,[6,7] screening of electrostatic interactions at high salt concentrations prevented the NPs of opposite polarities from aggregating (as indicated by UV−vis spectroscopy and dynamic light scattering (DLS) measurements; Figure 1B,C) and rendered the NP solutions stable for prolonged periods of time (up to months).

The NPs were gradually precipitated either by titration with small aliquots (~0.1 mL) of water (which contained only enough $N(CH_3)_4OH$ to maintain pH ≈ 11 conditions) or by increasing the temperature (from 10 to 40 °C). After each dilution or temperature increment, the solution was equilibrated while stirring for ~20 min, and the free NPs remaining in solution were analyzed by UV−vis and DLS. Since DLS showed only the presence of individual/unaggregated NPs, the concentration of dissolved NPs was determined from the intensity[13] of the maximum of the SPR absorption peak at ~518 nm.

Precipitation Trends

Figure 2B plots the concentration of NPs in solution (in terms of gold atoms) as a function of salt concentration during dilution for NP diameters, $D = 5.9$ nm and $D = 7.1$ nm. The largest particles ($D = 11$ nm) could not be dissolved—even at high salt concentrations owning to large van der Waals forces between the particles (cf. below). These plots indicate that the NPs are initially stable in solution until reaching a critical dilution, at which the dilution curve (diagonal lines in Figure 2B) intersects the NP solubility curve (solid lines in Figure 2B). Subsequently, nanoparticles begin to precipitate, and the degree of precipitation increases continuously with increasing dilution (i.e., with decreasing salt concentration). This precipitation is fully reversible, and when the solvent is evaporated (or when more salt is added), the NPs redisperse.

Figure 2C illustrates precipitation upon temperature increase. Here, we observe that the precipitation is reversible up to ~30 °C, and cooling causes redissolution of the NP precipitate. For higher temperatures, reversibility is not complete, likely due to the exchange[14] of MUA and TMA thiols between NPs in the precipitate.

Theoretical Analysis

i. Thermodynamics of the System. The reversibility of the precipitation/dissolution processes and the time independence

of NP concentrations at each titration point suggest that the observed phenomena may be understood using thermodynamic (i.e., not kinetic) arguments.[7] Thus, for a given salt concentration and temperature, free NPs in solution are in equilibrium with those in the aggregate phase (if present), and the measured NP concentration represents an equilibrium solubility.[15] The equilibrium between the dissolved (D) and aggregated (A) phases is determined by the equivalence of the NP chemical potentials, $\mu_D = \mu_A$,[16] which are assumed to obey the dilute-solution form, $\mu_i = \mu_i^\circ + kT \ln c_i$, where μ_i° and c_i are respectively the standard chemical potential and the concentration of NPs in phase i. Thus, the equilibrium NP solubility is approximated as

$$c_D = c_A \exp(\Delta\mu^\circ/kT) \quad (1)$$

where $\Delta\mu^\circ = \mu_A^\circ - \mu_D^\circ$ is the decrease in free energy associated with NP aggregation.

Inspecting the above relation for the NP solubility, one finds that c_D will decrease with dilution—as observed experimentally—only if the free energy of aggregation, $\Delta\mu^\circ$, also decreases (i.e., becomes more negative) at the same time. Similarly, $\Delta\mu^\circ$ must decrease faster than linearly with temperature in order for the NPs to precipitate upon increasing the temperature. To explain these phenomena, we must thus consider how the NP interactions governing $\Delta\mu^\circ$ depend on both salt concentration and temperature.

In the present system, the dominant contributions to $\Delta\mu^\circ$ are electrostatic (ES) and van der Waals (VDW) forces. In the dissolved phase, these forces are small since the mean interparticle distance (~140 nm for the unaggregated, dilute solutions used here) is much larger than the relevant length scales for both electrostatic (the screening length, $\kappa^{-1} \leq \sim 1$ nm) and van der Waals interactions ($|U_{VDW}| > kT$ only for $d - 2R_c \leq \sim 3$ nm; cf. below).[6,7] Consequently, $\mu_D^\circ \approx 0$ and $\Delta\mu^\circ \approx \mu_A^\circ$. On the other hand, in the aggregated phase, the proximal NPs interact strongly, and the total interaction energy may be approximated by a pairwise summation over nearest neighbors only. In this way, $\Delta\mu^\circ$ can be approximated as

$$\Delta\mu^\circ = \frac{1}{2} n(U_{ES} + U_{VDW}) \quad (2)$$

where U_{ES} and U_{VDW} are respectively the electrostatic and van der Waals interaction energies for two oppositely charged NPs at contact, and $n \sim 6$ is the average number of nearest neighbors in the aggregate phase estimated previously.[17]

ii. The van der Waals Energy. U_{VDW} is due primarily to the interactions between the NPs' metal cores and depends only negligibly on the salt concentration.[18] Specifically

$$U_{VDW} = -(A/3)\left[R_c^2/(d^2 - 4R_c) + R_c^2/d^2 + \frac{1}{2}\ln(1 - 4R_c^2/d^2)\right] \quad (3)$$

where $A = 4 \times 10^{-19}$ J is the Hamaker constant[18] for gold across water, R_c is the radius of the NP core, and $d = 2R = 2(R_c + \delta)$ is the distance between NP centers at contact (cf. Figure 3A), where $\delta \sim 1$ nm is the SAM thickness (estimated from TEM images and from previous X-ray diffraction results[8]). Thus, for the NPs described here (R_c = 2.95, 3.55, and 5.5 nm), the magnitude of the van der Waals interaction per NP pair is $|U_{VDW}| \approx 6 \times 10^{-21}$, 9×10^{-21}, and 24×10^{-21} J, respectively (or ~1.6kT, 2.3kT, and 6.0kT at room temperature).

iii. Electrostatic Interactions. Electrostatic interactions between charged NPs in equilibrium with an electrolyte solution are derived from the appropriate electrostatic potentials, φ, via thermodynamic integration[19,20] and account for "charge regulation" at the NPs' surfaces; that is, for the equilibrium between counterions adsorbed onto the charged surfaces and those "free" in solution (cf. Figure 3A).[7] Briefly, the electrostatic potential around the NPs or the substrate is well approximated[7] by the linearized Poisson−Boltzmann (PB) equation, $\nabla^2\varphi = \kappa^2\varphi$, where $\kappa^{-1} = (\varepsilon_0\varepsilon k_B T/2c_S e^2)^{1/2}$ is the Debye screening length, c_S is the monovalent salt concentration, e is the fundamental charge, ε_0 is the permittivity of vacuum, ε is the (temperature-dependent) dielectric constant of the solvent, k_B is Boltzmann's constant, and T is the temperature. The adsorption equilibrium at a positively charged surface (here, TMA-coated NPs) presenting N_T positively charged groups, A^+, in a solution containing negatively charged counterions, B^-, is determined by $N_{A^+}x_{B^-}/N_{AB} = \exp[-(\Delta G_d + e\varphi_s)/k_BT]$, where N_{A^+} and N_{AB} are respectively the numbers of counterion-free and counterion-bound surface ligands ($N_{A^+} + N_{AB} = N_T$), x_B is the mole fraction of counterions in solution, $\Delta G_d > 0$ is the free energy of ion dissociation in the absence of any external fields, and φ_s is the electrostatic potential at the surface. From this relation, the surface charge density, σ, may be expressed as $\sigma = e\Gamma/\{1 + x_{B^-}\exp[(\Delta G_d + e\varphi_s)/k_BT]\}$, where $\Gamma = N_T/4\pi R^2$ is the surface density of charged groups (e.g., $\Gamma \approx 4.7$ nm^{-2} for SAMs on gold NPs[21]). Considering that the dielectric constant of the SAM ($\varepsilon_p \approx 2$) is small compared to that of the solvent ($\varepsilon \approx 80$ for water), the surface charge is related to the potential at the NP surface by $\sigma = -\varepsilon_0\varepsilon\nabla\varphi\cdot\vec{n}$, where $\vec{n}$ is the outward surface normal. Equating the two relations for σ provides the necessary boundary condition for a positively charged NP. The boundary condition for negatively charged NPs is derived in a similar fashion, where it is assumed that the free energy of ion desorption, ΔG_d, is the same for both types of ligand−counterion pairs (i.e., MUA^-/NMe_4^+ and TMA^+/Cl^-).

To obtain an analytic form for the interaction energy, it is necessary to make two additional simplifying assumptions. In addition to linearizing the PB equation (appropriate for dimensionless potentials, $e\varphi/kT \leq 2$, described here), the boundary conditions at the NPs' surface are linearized about the potential of an isolated NP, φ_∞, such that $-\varepsilon_0\varepsilon\nabla\varphi\cdot\vec{n} = S - C\varphi$, where $S = \sigma(\varphi_\infty) - (\partial\sigma/\partial\varphi)_\infty\varphi_\infty$ and $C = -(\partial\sigma/\partial\varphi)_\infty$.[22] Furthermore, at the salt concentrations of interest (here, $c_S \sim 1$ M) the screening length is much smaller than the NP radius, $\kappa R \gg 1$; therefore, it is appropriate to apply the Derjaguin approximation,[18,20] which simplifies the bispherical geometry to a simple planar geometry. With these assumptions, the interaction energy between two like-sized NPs (1 and 2) at contact is given by

$$U_{ES} = \pi\varepsilon_0\varepsilon R\left[\frac{(\varphi_2^\infty)^2 + (\varphi_1^\infty)^2}{2\Delta}\ln(1 - \Delta^2) + \frac{2\varphi_1^\infty\varphi_2^\infty}{\Delta}\operatorname{atanh}(\Delta)\right] \quad (4)$$

where $\Delta = (C - \varepsilon_0\varepsilon\kappa)/(C + \varepsilon_0\varepsilon\kappa)$.[19] Figure 3B illustrates the dependence of the electrostatic interaction energy, U_{ES}, on both the salt concentration and the temperature for two oppositely charged NPs at contact: the interactions become stronger with decreasing salt concentration or with increasing temperature. Likewise, ζ-potential measurements of positive TMA particles

and negative MUA particles reveal that the surface potentials of isolated particles, φ^{∞}, also increase in magnitude with decreasing salt concentration or with increasing temperature (cf. Figure 3C).

Results and Discussion

i. Theoretical Solubility Curves. Substituting electrostatic and van der Waals energies (eqs 3 and 4, respectively) into the expression for $\Delta\mu^{\circ}$ (eq 2), the theoretical solubility dependence—as a function of both salt concentration, c_S, and temperature, T—is obtained through eq 1. This dependence captures the decrease in NP solubility with decreasing c_S (i.e., with increasing dilution) and with increasing T. In fitting the generic formula to the actual experimental data (cf. fitted curves and experimental markers in Figure 2B,C), the only free parameters are the free energy of ion desorption, ΔG_d, and the core−core separation distance, d, used in calculating the van der Waals energy, U_{VDW}. Best-fit values of $\Delta G_d \approx 2.1 \times 10^{-20}$ J (13 kJ/mol) and $d \approx 7.7$ and 9.0 nm (for NP core diameters 5.9 and 7.1 nm, respectively) were estimated by minimizing the sum squared error, between experimental and calculated NP solubilities, $\chi^2 = \sum[\ln(c_D^{exp}) - \ln(c_D^{calc})]^2$, using the simplex search method.[23] These values are physically reasonable. For example, the dissociation energy, ΔG_d, is comparable to the Coulombic interaction energy between oppositely charged, monovalent ions, $\Delta G_d \approx e^2/4\pi\varepsilon_0\varepsilon D$, where D is a characteristic ionic diameter. Indeed, for $D = 3.6$ Å (as for Cl^-), $e^2/4\pi\varepsilon_0\varepsilon D \approx 1 \times 10^{-20}$ J, which differs only by a factor of 2 from the experimental estimate of ΔG_d. Furthermore, when this best-fit value is used to estimate the surface potentials of the isolated particles, the results agree well with those of ζ-potential experiments (cf. dashed curves in Figure 3C). Likewise, the best-fit values of d correspond to SAM thicknesses (at contact) of $\delta \approx 0.9$ nm and $\delta \approx 1.0$ nm for 5.9 and 7.1 nm particles, respectively, in strong agreement with previous estimates. These values correspond to van der Waals energies of $U_{VDW} \approx 8.1 \times 10^{-21}$ J and $U_{VDW} \approx 1.0 \times 10^{-20}$ J ($\sim 2.0kT$ and $\sim 2.4kT$ at room temperature).

ii. Origin of Solubility/Precipitation Trends. The fact that mixtures of small (here, 5.9 and 7.1 nm), oppositely charged NPs can be completely dissolved at high salt concentrations is the result of (i) a decrease in the magnitude of electrostatic interactions with increasing salt concentration and (ii) weak vdW forces, which alone are insufficient to cause aggregation. Unlike most colloidal dispersions (e.g., of lyophobic particles,[20] proteins,[24] or DNA[25]), which are stabilized by *repulsive* electrostatic interactions and aggregate only upon *addition* of salt, the present system is characterized by strong attractive electrostatic interactions, which must be eliminated to enable dissolution. Here, the role of salt is twofold: some ions adsorb onto the charged terminal groups of the thiols stabilizing the NPs, thereby reducing the effective charge of the particles;[26] meanwhile, ions in the diffuse double layer screen electrostatic interactions between neighboring NPs. Both effects serve to weaken electrostatic interactions between particles.

Upon dilution, the accompanying decrease in the salt concentration serves to strengthen the electrostatic attraction between oppositely charged NPs (cf. Figure 3B, left), thereby decreasing their solubility. Specifically, the salt concentration enters the calculation of $\Delta\mu^{\circ}$ in two ways. First is through the screening length, κ^{-1}, which decreases as one over the square root of c_S. Thus, electrostatic interactions become more long ranged with decreasing salt concentration, thereby increasing the magnitude of electrostatic interactions—even those between nearest neighbors.[27] More important, however, is the influence of the salt concentration at the NP surface, where the local charge density depends on the mole fraction of salt, x_S, as $\sigma = e\Gamma/\{1 + x_S \exp[(\Delta G_d + e\varphi_s)/k_BT]\}$, which is a monotonically decreasing function of the salt concentration. In other words, decreasing the salt concentration facilitates desorption of ions from the NPs' surfaces, thereby increasing the effective charge of the particles and the magnitude of their electrostatic interactions.[28,29]

Similarly, an increase in temperature also leads to desorption of ions from the NPs, resulting in stronger electrostatic attraction between the particles and a decrease in particles' solubility (cf. Figure 3B, right). As in the case of varying salt concentration, temperature enters predominantly through the ion-adsorption equilibria at the NPs' surfaces. While the temperature also enters through the screening length, κ^{-1}, this effect is largely negated by the temperature dependence of the dielectric constant of water; consequently, the screening length is approximately temperature independent. By contrast, owing to the ion-adsorption equilibria, the local charge density at the NP surfaces increases significantly with increasing temperature due to the desorption of ions and resulting in stronger electrostatic interactions. It is worth noting, however, that simply increasing the magnitude of NP interactions with increasing T is not a sufficient condition to achieve NP precipitation. Instead, the magnitude of U_{ES} must increase faster than linearly with T such that $|\Delta\mu^{\circ}(T)/kT|$ is a monotonically increasing function of T, and c_D decreases with T (cf. eq 1).

Finally, in addition to salt concentration and temperature, particle size also has a dramatic effect on NP solubility. Specifically, the magnitudes of both the electrostatic and van der Waals interactions increase with increasing particle size—the former increasing roughly linear with particle diameter (at least for $\kappa R \gg 1$) while the latter increases faster than linearly.[7] Thus, for larger particles, such as the 11 nm NPs used here, the van der Waals interaction ($\sim 6kT$) becomes sufficiently strong as to cause precipitation even in the absence of additional electrostatic forces.

Conclusions

In summary, we described and explained the precipitation of oppositely charged NPs upon dilution and/or temperature increase. This phenomenon illustrates the importance of counterion desorption for the stability of suspensions of charged nano-objects. Understanding these effects has practical ramifications for the preparation of coatings[6,30] and nanostructured materials[8,31,32] from "ionic" nanoparticles of opposite polarities.[6−10,30] In the future, it would be interesting to study solubility/precipitation (and maybe even self-assembly) of nonspherical nanoobjects[33] where the particles' geometry would translate into nonuniform surface potentials (especially, around sharp corners) and potentially into "directional" electrostatic interactions. Also, extension to systems of microscopic particles is intriguing albeit in this case minimization of vdW forces (necessary to prevent indiscriminate aggregation) by nonaqueous, index-matching solvents might limit the ability to tailor and control the system's electrostatics over a wide range of salt concentrations/temperatures.

References and Notes

(1) Moren, A. K.; Khan, A. *Langmuir* **1998**, *14*, 6818.
(2) Macritc, F. *J. Colloid Interface Sci.* **1973**, *45*, 235.
(3) Bailey, F. E.; Callard, R. W. *J. Appl. Polym. Sci.* **1959**, *1*, 56.
(4) Napper, D. H. *J. Colloid Interface Sci.* **1970**, *33*, 384.
(5) In this paper, we refer to NP "solutions" as opposed to NP "suspensions" because the dispersed NPs are thermodynamically (not just

kinetically) stable against sedimentation for the length scales considered here. Specifically, experiments were performed on solutions ~2 cm in height, which is small compared to the gravitational length scale $L_g = kT/m_{NP}g \approx 20$ cm, where kT is the thermal energy, m_{NP} is the mass of an NP (relative to the solvent it displaces), and g is the acceleration due to gravity.

(6) Smoukov, S. K.; Bishop, K. J. M.; Kowalczyk, B.; Kalsin, A. M.; Grzybowski, B. A. *J. Am. Chem. Soc.* **2007**, *129*, 15623.

(7) Bishop, K. J. M.; Grzybowski, B. A. *ChemPhysChem* **2007**, *8*, 2171.

(8) Kalsin, A. M.; Fialkowski, M.; Paszewski, M.; Smoukov, S. K.; Bishop, K. J. M.; Grzybowski, B. A. *Science* **2006**, *312*, 420.

(9) Kalsin, A. M.; Grzybowski, B. A. *Nano Lett.* **2007**, *7*, 1018.

(10) Kalsin, A. M.; Kowalczyk, B.; Smoukov, S. K.; Klajn, R.; Grzybowski, B. A. *J. Am. Chem. Soc.* **2006**, *128*, 15046.

(11) Kalsin, A. M.; Kowalczyk, B.; Wesson, P.; Paszewski, M.; Grzybowski, B. A. *J. Am. Chem. Soc.* **2007**, *129*, 6664.

(12) Leopold, M. C.; Black, J. A.; Bowden, E. F. *Langmuir* **2002**, *18*, 978.

(13) Bohren, C. F.; Huffman, D. R. *Absorption and Scattering of Light by Small Particles*; Wiley & Sons Inc.: New York, 1998.

(14) Zachary, M.; Chechik, V. *Angew. Chem., Int. Ed.* **2007**, *46*, 3304.

(15) Of course, in the absence of NP aggregates (i.e., the concentration of NPs is below the solubility curve), there is no such equilibrium, and the number of dissolved NPs is independent of both dilution and temperature (cf. Figure 1B).

(16) Because the positively and negatively charged NPs are equally sized and symmetric with respect to their charges, it is assumed that their chemical potentials are also equivalent, i.e., $\mu_+ = \mu_-$.

(17) Pinchuk, A. O.; Kalsin, A. M.; Kowalczyk, B.; Schatz, G. C.; Grzybowski, B. A. *J. Phys. Chem. C* **2007**, *111*, 11816.

(18) Israelachvili, J. N. *Intermolecular and Surface Forces*, 2nd ed.; Academic Press: New York, 1991.

(19) Carnie, S. L.; Chan, D. Y. C.; Gunning, J. S. *Langmuir* **1994**, *10*, 2993.

(20) Verwey, E. J. W.; Overbeek, J. T. G. *Theory of the Stability of Lyophobic Colloids*; Elsevier: New York, 1948.

(21) Leff, D. V.; Ohara, P. C.; Heath, J. R.; Gelbart, W. M. *J. Phys. Chem.* **1995**, *99*, 7036.

(22) For an isolated NP with the "charge regulating" boundary condition, solution of the linear PB equation gives the relation $e\Gamma/\{1 + x_{B^-} \exp[(\Delta G_d + e\varphi_\infty)/k_BT]\} = \varepsilon_0\varepsilon\varphi_\infty(1 + \kappa R)/R$, which may be solved numerically for the surface potential at infinite separation, φ_∞.

(23) Lagarias, J. C.; Reeds, J. A.; Wright, M. H.; Wright, P. E. *SIAM J. Optim.* **1998**, *9*, 112.

(24) Coen, C. J.; Blanch, H. W.; Prausnitz, J. M. *AIChE J.* **1995**, *41*, 996.

(25) Raspaud, E.; de la Cruz, M. O.; Sikorav, J. L.; Livolant, F. *Biophys. J.* **1998**, *74*, 381.

(26) Belloni, L. *Colloids Surf., A* **1998**, *140*, 227.

(27) For small screening lengths, the effective area of interaction between two NPs at contact can be estimated as $2\pi R\kappa^{-1}$ (cf. ref 18); thus, increasing the screening length, κ^{-1}, increases the area of interaction and thereby the magnitude of electrostatic interactions.

(28) It is worth noting that because ions desorb from the NPs both upon dilution and upon NP aggregation (e.g., see ref 28), the total number of dissolved ions (i.e., those not adsorbed onto the NPs) actually increases with increasing dilution, while the number of dissolved NPs decreases. With these considerations, dilution has the intuitive effect of increasing the total number of dissolved species (both ions and NPs) in solution.

(29) Meier-Koll, A. A.; Fleck, C. C.; von Grunberg, H. H. *J. Phys. Condens. Matter* **2004**, *16*, 6041.

(30) Lee, D.; Rubner, M. F.; Cohen, R. E. *Nano Lett.* **2006**, *6*, 2305.

(31) Redl, F. X.; Cho, K. S.; Murray, C. B.; O'Brien, S. *Nature (London)* **2003**, *423*, 968.

(32) Shevchenko, E. V.; Talapin, D. V.; Kotov, N. A.; O'Brien, S.; Murray, C. B. *Nature (London)* **2006**, *439*, 55.

(33) Klajn, R.; Pinchuk, A. O.; Schatz, G. C.; Grzybowski, B. A. *Angew. Chem., Int. Ed.* **2007**, *46*, 8363.

JP8056493